

Exploiting Inexact Computations in Multilevel Sampling Methods

Josef Martínek*, Erin Carson†, Robert Scheichl*

March 20, 2025

Abstract

Multilevel sampling methods, such as multilevel and multifidelity Monte Carlo, multilevel stochastic collocation, or delayed acceptance Markov chain Monte Carlo, have become standard uncertainty quantification tools for a wide class of forward and inverse problems. The underlying idea is to achieve faster convergence by leveraging a hierarchy of models, such as partial differential equation (PDE) or stochastic differential equation (SDE) discretisations with increasing accuracy. By optimally redistributing work among the levels, multilevel methods can achieve significant performance improvement compared to single level methods working with one high-fidelity model. Intuitively, approximate solutions on coarser levels can tolerate large computational error without affecting the overall accuracy. We show how this can be used in high-performance computing applications to obtain a significant performance gain.

As a use case, we analyse the computational error in the standard multilevel Monte Carlo method and formulate an adaptive algorithm which determines a minimum required computational accuracy on each level of discretisation. We show two examples of how the inexactness can be converted into actual gains using an elliptic PDE with lognormal random coefficients. Using a low precision sparse direct solver combined with iterative refinement results in a simulated gain in memory references of up to $3.5\times$ compared to the reference double precision solver; while using a MINRES iterative solver, a practical speedup of up to $1.5\times$ in terms of FLOPs is achieved. These results provide a step in the direction of energy-aware scientific computing, with significant potential for energy savings.

Keywords. multilevel, Monte Carlo, mixed precision, iterative refinement, energy-efficient computing.

Mathematics Subject classifications. 65Y20, 65C05, 65C30, 65G20, 60-08.

1 Introduction

Suppose we are interested in sampling from a probability distribution of a certain quantity Q , which depends on the (infinite-dimensional) solution of a partial differential equation (PDE) or a stochastic differential equation (SDE). In most cases, direct access to Q is unavailable. Instead, a numerical model is used to obtain a finite-dimensional approximation Q_L of the quantity Q . With increasing L the accuracy of the model increases, but so does the cost of computing the solution. This can be a finite element or finite difference method in the case of PDEs, or an Euler-Maruyama discretisation for SDEs. A first idea to approximate the unavailable distribution of Q is to choose a high-fidelity model Q_L with L sufficiently

*Institute for Mathematics and Interdisciplinary Center for Scientific Computing (IWR), Heidelberg University, 69120, Heidelberg, Germany (martinek@math.uni-heidelberg.de, r.scheichl@uni-heidelberg.de)

†Department of Numerical Mathematics, Faculty of Mathematics and Physics, Charles University, Sokolovská 49/83, 186 75 Praha 8, Czechia (carson@karlin.mff.cuni.cz)

large and to use this model for sampling. Instead, the key idea of multilevel and multifidelity sampling methods, such as multilevel Monte Carlo (MLMC) [15], multilevel stochastic collocation [30], or delayed acceptance MCMC [9], is to use a hierarchy of models Q_0, \dots, Q_L with increasing accuracy. Then, by combining all the samples from models Q_0, \dots, Q_L in a suitable way, a significant cost gain can be achieved.

Convergence of the aforementioned multilevel schemes has been thoroughly studied in various settings. The analysis is typically concerned with balancing the sampling and bias error to achieve an optimal performance. This paper adds one additional layer to the analysis, which has, to our knowledge, largely been neglected. In practice, the finite-dimensional model Q_l is never solved exactly, rather an approximation \tilde{Q}_l is obtained on a computer. We show that multilevel methods often admit safe use of inexact computations on coarse levels l without affecting overall sampling accuracy. An elegant way to achieve the given low accuracy of the inexact solution \tilde{Q}_l is the use of iterative procedures, such as Krylov subspace methods or iterative refinement. Efficient implementation of these techniques may lead to significant gains in terms of both time and energy in high performance computing applications [19, 18, 5].

To give a concrete example, we consider the MLMC method and rigorously show how the required computational accuracy is tied to the model accuracy at level l . We further establish a theoretical framework for quantifying the computational error by choosing a suitable error model. To fully leverage it, one needs to determine where the dominant computational cost lies. In many models the dominant cost lies in the solution of linear algebraic equations, which is why, for our case study, we choose an uncertainty quantification problem given by an elliptic PDE with lognormal random coefficients. Another example, recently studied in [16], addresses the cost of generating random variables, which can also be significant in some cases.

With this motivation in mind, we will consider a *model problem* of the form

$$-\nabla \cdot (a(\cdot, \omega) \nabla u(\cdot, \omega)) = f(\cdot, \omega).$$

An elliptic PDE of this form depending on a random parameter ω arises, for example, in uncertainty quantification of groundwater flow [10]. We are interested in estimating the value of a quantity of interest (QoI), given as a function G of the solution u , such as the expected value of a given functional of the solution, e.g., the expected value of the value of the solution at a certain point in the domain. The coefficient a and the right-hand side f are assumed to be (infinite-dimensional) random fields. In practice, they also have to be approximated and depend on a high-dimensional random parameter vector ω . Due to the high-dimensionality, the numerical approximation of the quantity of interest becomes exponentially difficult, which is known as the *curse of dimensionality*; see, e.g., [15, 27].

Thus we are interested in sampling from the unavailable distribution of the quantity $Q = G(\omega)$ to compute statistics of this distribution, e.g., the mean $\mathbb{E}[Q]$. To obtain a computable approximation Q_L of Q we choose the finite element method (FEM). This introduces in our approximation the so-called discretisation error, referred to also as model error or bias. After the PDE has been discretised, we have to face the challenge of approximating $\mathbb{E}[Q_L]$. To this end, Monte Carlo (MC) methods are often used, which introduces a sampling error. In the standard Monte Carlo method we need to take a sufficient number of samples of the discrete solution computed on a sufficiently fine mesh in order to bound both the sampling and the discretisation error. A significant variance reduction can be achieved if the samples are taken on a hierarchy of discretisation levels. This is the underlying idea of the MLMC method [20, 10, 15]. The MLMC method dramatically reduces the variance of the resulting estimator while preserving the overall cost and it allows us to efficiently balance the two errors — discretisation error and sampling error.

In our model problem, four main numerical procedures have to be performed. The first is sampling the random fields $a(\cdot, \omega)$ and $f(\cdot, \omega)$, $\omega \in \Omega$; the second is assembling the FE stiffness matrix; the third corresponds to solving the associated linear system; and the final one involves computing the MLMC estimate itself. In our case, the cost of sampling random variables is small, and so is the cost of computing the MLMC estimate itself. Moreover, using inexact computations to compute the MLMC estimate could result in violating the MLMC telescopic property, so it is not of great interest. The stiffness matrix assembly

cost may be significant, but it can be implemented in linear complexity (see, for example, [33]), so that it is not asymptotically dominant. Nevertheless, efficient implementation of the stiffness matrix assembly may also be of interest and bring a significant reduction in solution time. However, in this work, we focus on the dominant cost of solving the resulting linear system and how to reduce it using inexact computations. The error introduced by solving the linear system will be referred to as the computational error. It stems from the fact that the system is solved with an inexact linear solver, yielding an approximate solution \tilde{Q}_l of the model Q_l , as discussed above. To balance the computational error with the sampling and discretisation errors, we determine the minimum computational accuracy required for solving the linear system, which is a general solver-independent result. In practice, how inexact computations can be exploited depends on the particular solver.

To demonstrate the flexibility of our approach, we consider both direct and iterative solvers and discuss how to exploit inexactness in each of them. For iterative solvers, we suggest to determine the optimal number of iterations via a suitable stopping criterion. For direct solvers, we use mixed precision arithmetic and employ the technique of iterative refinement; cf. [21, 32]. In recent years, there has been growing interest in the selective use of low precision floating point arithmetic to accelerate scientific computations while maintaining acceptable levels of accuracy; cf. [22].

There are a couple of works that go in the direction of this manuscript. In [4], the authors explore the use of lower precision on field programmable gate arrays (FPGA) in the MLMC method, using a stochastic differential equation (SDE) discretised by the Euler method as the model problem. The recent paper by Giles and Sheridan-Methven [16] is concerned with the analysis of rounding errors in generating random variables in the context of SDEs, again with application to multilevel Monte Carlo. We approach this topic from a different perspective. Namely, we

- establish a theoretical framework for quantifying the computational error in the MLMC method by choosing a suitable error model (Section 4.2);
- propose a novel adaptive algorithm, determining the minimum required computational accuracy on each level of discretisation using a-priori error estimates with no additional cost (Section 4.4);
- provide a theoretical basis for applying the adaptive algorithm to the model elliptic PDE with random coefficients and a random right-hand side (Section 4.3);
- demonstrate the efficiency of the adaptive algorithm through a sequence of numerical examples, achieving up to a factor of about $3.5\times$ in simulated memory gain with iterative refinement and a speedup by a factor of about $1.5\times$ in terms of floating point operations with an iterative solver. A cost analysis and possible use in energy-efficient scientific computing are presented in Section 4.5.

The manuscript is divided into five sections. In the second section, we discuss linear solvers and various types of errors induced by their use. We give an overview of floating point arithmetic, the technique of iterative refinement, as well as some convergence results of Krylov subspace methods. The third section introduces the elliptic model problem, as well as its numerical solution by finite elements. Selected FE convergence results are presented and the convergence of the FEM using inexact solvers is discussed. In the fourth section we give a brief overview of the standard MLMC method, and the novel analysis of the computational error in MLMC along with the adaptive algorithm and the cost analysis. Finally, the numerical results along with a thorough discussion are given in Section 5.

2 Linear solvers and inexact computations

Let \hat{x} be a solution of a linear system $Ax = b$ computed by an algorithm. The solution is said to be computed effectively to precision δ_e if

$$\frac{\|b - A\hat{x}\|_2}{\|b\|_2} \leq C\delta_e \quad (1)$$

for a constant $C > 0$. Here $\|\cdot\|_2$ denotes the Euclidean norm, although it is possible to use any other norm in principle. The constant C may or may not be dependent on the matrix A and other input data; this is problem-dependent.

2.1 Floating point arithmetic

A floating point (FP) number system \mathbb{F} is a finite subset of real numbers whose elements can be written in a specific form; see [21] for a thorough description. All computations in FP arithmetic are assumed to be carried out under the following standard model: For all $x, y \in \mathbb{F}$

$$fl(x \text{ op } y) = (1 + \nu)(x \text{ op } y), \quad |\nu| \leq \varepsilon, \quad \text{op} = +, -, \times, /, \quad (2)$$

where ε is the unit roundoff. This assumption allows us to analyse the error of a given algorithm. For simplicity, we will often abbreviate “the floating point arithmetic format with unit roundoff ε ” to “the precision ε ”.

The standard model is valid in particular for IEEE arithmetic, a technical standard of floating point arithmetic, which assumes the preliminaries above and adds other technical assumptions; see [21] for an overview. The IEEE standard defines several basic formats. In this work, we use formats both standardized and not standardised by IEEE. All of the formats we will use are hardware-supported, namely by the NVIDIA H100 SXM GPU (for specifications see [28]). To be specific, in this manuscript we use quarter (q43), half, single, and double precision. Half, single, and double are basic IEEE formats. The quarter precision format we use has 4 exponent bits and 3 significand bits, which means storing one number requires 8 bits including the sign. The unit roundoff of quarter precision is 2^{-4} and its range is $10^{\pm 2}$.

Not all arithmetic operations in an algorithm need to be carried out in the same precision. There are techniques which allow us to improve the accuracy of the computed solution via, e.g., iterative refinement, discussed in Section 2.3. Moreover, the theoretical error estimates of numerical methods often exaggerate the true error. This motivates us to introduce the so-called effective precision δ_e in (1), which is not necessarily a hardware or software-supported precision (e.g., like the IEEE standards). It is rather a parameter expressing how accurately the solution is actually computed.

2.2 Krylov subspace methods

Krylov subspace methods are a powerful class of iterative methods used for solving large-scale linear systems of equations and eigenvalue problems, particularly those involving sparse or structured matrices. Our application yields matrices which are symmetric positive definite (see Section 3), which makes the conjugate gradient (CG) and MINRES methods two suitable Krylov subspace methods for our purpose. The following overview of the methods is adapted from [17, Section 3.1].

Consider a linear system $Ax = b$ with symmetric positive definite $A \in \mathbb{R}^{n \times n}$. Let $x_0 \in \mathbb{R}^n$ be an initial estimate of the solution, $e_0 = x - x_0$ the initial error, and $r_0 = b - Ax_0$ the initial residual. Then, in each iteration k , CG minimizes the A -norm of the error and MINRES minimizes the Euclidean norm of the residual over the Krylov subspace $x_0 + \text{span}\{r_0, A^2r_0, \dots, A^{k-1}r_0\}$.

The stopping criterion we set is given by the relative residual and is motivated by our specific use of the linear solver; see Sections 4.2 and 5. To be precise, we require the solution produced by the iterative algorithm to satisfy (1) for a given $\delta_e > 0$. This motivates our choice to use the MINRES method in this work. It has been shown that residuals produced by the CG and MINRES methods on Hermitian matrices are closely related (see [17, Exercise 5.1]), and therefore both methods are expected to perform well for our model problem to be introduced in Section 3. Using the stopping criterion given by the relative residual will allow us to apply abstract error estimates from Section 4.2 to MINRES.

It is clear that in exact arithmetic, MINRES converges to the true solution in a finite number of iterations. In finite precision arithmetic, this is not the case, and the convergence analysis is nontrivial;

see for example [17, Chapter 4]. We therefore perform all calculations in the MINRES method in double precision. In order to apply the abstract error estimates from Section 4.2 to MINRES, we assume $\hat{x}_k \approx x_k$, where \hat{x}_k and x_k are the MINRES solutions from k -th iteration computed in floating point and exact arithmetic, respectively. An alternative approach to performing all calculations in high precision would be to employ a Krylov subspace method coupled with iterative refinement; see Section 2.3 for an overview of iterative refinement. Iterative refinement as a technique to improve accuracy of a Krylov subspace method was used, for example, in [6] and [7] with the GMRES method.

2.3 Iterative refinement

Iterative refinement is a technique used to enhance the accuracy of a numerical solution to a linear system by computing a residual vector and then applying a correction to the current approximation to reduce the error; see [21, Section 12] for a detailed overview. In this way, the process can be repeated iteratively until the limiting level of accuracy is achieved. The particular version of iterative refinement which we use in this work is adapted from [7]. Consider a linear system $Ax = b$ where $A \in \mathbb{R}^{n \times n}$ and $b \in \mathbb{R}^n$. The iterative refinement algorithm works explicitly with the following three precisions:

- ε is the (working) precision at which the data A , b and solution x are stored,
- ε_f is the precision at which the factorisation of A is computed,
- ε_r is the precision at which residuals are computed.

Implicitly, the algorithm contains a fourth precision, ε_s , which is the precision at which the correction equation is effectively solved. Note that in this subsection the symbol ε_s does not denote single precision and we use it here to keep the indices in accordance with [7], where the precision are denoted by u_r , u , u_f , and u_s , respectively.

All of the precisions ε_r , ε , ε_s , and ε_f will take, in the cases of interest, one of the values of quarter, half, single, or double precision, and it is assumed $\varepsilon_r \leq \varepsilon \leq \varepsilon_s \leq \varepsilon_f$. We present Algorithm 2.1 which is a special case of [7, Algorithm 1.1]. As mentioned above, ε_s is the precision at which the equation in step 8 is solved. In our case, $\varepsilon_s = \varepsilon_f$, since the factorisation is carried out in precision ε_f and we always consider the factorisation method to be the Cholesky decomposition.

Algorithm 2.1 Iterative refinement

Require: $A \in \mathbb{R}^{n \times n}$, $b \in \mathbb{R}^n$, both in precision ε , tolerance $\delta_e > 0$.

Ensure: an approximation x_i of the solution x stored in precision ε .

- 1: Factorise A in precision ε_f .
 - 2: Solve $Ax_0 = b$ in precision ε_f by substitution and store x_0 at precision ε .
 - 3: **for** $i = 0$ to i_{\max} **do**
 - 4: Compute $r_i = b - Ax_i$ at precision ε_r and round r_i to precision ε_s .
 - 5: **if** $\|r_i\|/\|b\| < \delta_e$ **then**
 - 6: Exit algorithm.
 - 7: **end if**
 - 8: Solve $Ad_i = r_i$ by (forward/backward) substitution at precision ε_f or ε using the factorisation computed in step 1 and store d_i at precision ε .
 - 9: $x_{i+1} = x_i + d_i$ at precision ε .
 - 10: **end for**
-

The precision to be used in step 8 of the algorithm is always specified when iterative refinement is used. By using a precision higher than the factorisation precision in step 8 of the algorithm, i.e., $\varepsilon_s < \varepsilon_f$, no numerical benefit from the perspective of the limiting tolerance for the residual norm $\|r_i\|/\|b\|$ can be

obtained. However, it turns out that using higher precision in step 8 can help us in practice to reach the same desired tolerance faster with a small additional cost. In our case, there is also no reason to use extra precision to compute the residual in step 4 of the algorithm, since we are only interested in bounding the backward error. Computing the residual in higher precision is useful if bounding the forward error is of interest; see [7].

In this work we use Algorithm 2.1 extensively to achieve the desired accuracy of the computed solution. We obtain additional benefits from using iterative refinement in terms of the cost. The point is to reuse the factorisation computed in step 1 of the algorithm in step 8 of the algorithm. If we reuse the factorisation as suggested, we can improve the accuracy of the solution with a small additional cost, because the factorisation is typically the dominant part in terms of the required number of operations; see [32, Section 2.2].

The stopping criterion in Algorithm 2.1, similarly as in Krylov subspace methods, is given by the relative residual norm. It is again motivated by our specific use of iterative refinement; see Sections 4.2 and 5. From the definition of the stopping criterion in step 5 it follows that if Algorithm 2.1 converges, then the produced solution is computed effectively to precision δ_e in the sense of (1). This will allow us to apply abstract error estimates from Section 4.2 to iterative refinement. The convergence of Algorithm 2.1 is analysed thoroughly in [7].

The convergence properties of iterative refinement for linear systems stemming from finite element discretisations of elliptic PDEs will be investigated in Section 3.2.

2.4 Energy savings through iterative refinement

We finish this section by discussing how using low precision can translate into energy or runtime savings. In the past decades, power has become the principal constraint of computing performance [25]. On the hardware level, this has led to the development of domain specific accelerators which enhance computing performance for specific applications [12, 26]. On the software level, attention has recently been brought to energy-aware algorithms for scientific computing. Mixed precision iterative refinement has successfully been applied in this area.

In [19], the potential for using iterative refinement in designing energy-efficient linear solvers was studied in the context of the LU factorisation of a dense matrix. The FP16-TC dghesv-TC (Tensor Cores) solver using iterative refinement and half precision for the matrix factorisation achieved more than $5\times$ improvement in terms of energy efficiency than then standard dgesv routine which factorises the matrix in double precision with no iterative refinement.

In [18], several numerical experiments measuring the performance gain of low precision arithmetic were conducted using an NVIDIA V100 PCIe GPU. The LAPACK algorithm GETRF for computing the LU factorisation of a dense matrix was studied in various precisions. Their implementation computing the LU factorisation accurately to half precision using TC achieves a speedup of $4\times$ to $5\times$ compared to double precision and a $2\times$ speedup over single precision (both not using Tensor Cores).

In our experiments, we obtained a simulated gain of up to $\approx 3.5\times$ in terms of memory references; see Figure 6. The ratio of the cost of a memory access to the cost of a floating point operation is continuing to grow in recent architectures [26, Table 2]. On modern 7nm semiconductor architectures, a cache (SRAM) memory access is on average $10\times$ to $100\times$ more expensive in terms of energy than a floating point operation. At the same time, accessing SRAM is up to $100\times$ cheaper than accessing DRAM. Therefore, an efficient parallel implementation of iterative refinement within the proposed adaptive algorithm (Algorithm 4.1) that allows one to store more data in the cache memory can bring a significant reduction in energy cost, which is a promising area for future research.

3 Finite element methods for PDEs with random data

As a use case for inexact computations within multilevel sampling methods, we now consider the multilevel Monte Carlo method and a standard elliptic PDE with random data discretised via finite elements (FE). Problems of this kind arise, for example, in geosciences, namely, in the study of groundwater flow; see [29, 24, 14], and the references therein.

3.1 An elliptic PDE with random data and its FE solution

We now state the standard weak formulation of an elliptic PDE with random data:

Problem 3.1 (AVP with random data). Let $(\Omega, \mathcal{U}, \mathbb{P})$ be a probability space and $V := H_0^1(D)$ where D is a bounded domain in \mathbb{R}^d , $d = 2, 3$. For $\omega \in \Omega$, we define $\mathcal{A} : V \times V \times \Omega \rightarrow \mathbb{R}$ and $l : V \times \Omega \rightarrow \mathbb{R}$ by

$$\begin{aligned} \mathcal{A}(u(\cdot, \omega), v, \omega) &:= \int_D a(x, \omega) \nabla u(x, \omega) \cdot \nabla v(x) dx \quad \text{and} \\ l(v, \omega) &:= \int_D f(x, \omega) v(x) dx, \end{aligned} \tag{3}$$

respectively, where a and f are fixed random fields satisfying $a(\cdot, \omega) \in L^\infty(D)$ and $f(\cdot, \omega) \in L^2(D)$. A function $u(\cdot, \omega) \in V$ is a solution of this *abstract variational problem* if it satisfies for a.e. $\omega \in \Omega$

$$\mathcal{A}(u(\cdot, \omega), v, \omega) = l(v, \omega) \quad \text{for all } v \in V.$$

In order to prove the unique solvability of the AVP with random data, we assume that there exist a_{min} and a_{max} such that

$$0 < a_{min} \leq a(x, \omega) \leq a_{max} < \infty \quad \text{for a.e. } \omega \in \Omega \quad \text{and a.e. } x \in D. \tag{4}$$

Under the assumption (4) the unique solvability of the AVP with random data (Problem 3.1) can be proved sample-wise using the Lax-Milgram lemma in the standard way; see [1]. The coercivity and continuity constants in the Lax-Milgram lemma do not depend on ω . More details regarding the analysis of Problem 3.1 in the stochastic context can be found in [1, 3]. Let us note that if the bounds in (4) are weakened and depend on ω , the analysis is still possible but it becomes more complicated; see [31] for a thorough discussion.

To obtain a FE error estimate in the L^2 norm, the domain D is assumed to be convex and the random field a is assumed to be uniformly Lipschitz continuous, i.e., there exists $L > 0$ such that

$$|a(x_1, \omega) - a(x_2, \omega)| \leq L \|x_1 - x_2\| \quad \text{for a.e. } \omega \in \Omega \quad \text{and a.e. } x_1, x_2 \in D. \tag{5}$$

In order to solve Problem 3.1, we use conforming FEs on a shape-regular and quasi-uniform family of triangulations of the domain $D \subset \mathbb{R}^n$ (in our examples $n = 2$) with a mesh parameter $h > 0$. We employ (piecewise linear) \mathcal{P}_1 Lagrange elements to compute the *discrete solution* $u_h(\cdot, \omega)$ to the AVP with random data (Problem 3.1) in the FE space $V_h \subset V$. Using a basis of V_h consisting of hat functions ϕ_j , this is equivalent to solving a linear system $A(\omega)x(\omega) = b(\omega)$ with a positive definite matrix $A(\omega)$; see [13] for details.

3.2 Approximate FE solutions using inexact solvers

Due to the limitations of inexact linear solvers, the discrete solution u_h is not obtained exactly in practice. Instead, we compute an approximation \hat{u}_h . The aim of this section is to estimate the error $\|u_h(\cdot, \omega) - \hat{u}_h(\cdot, \omega)\|_{H_0^1(D)}$ by means of the residual of the solution of the FE system $Ax = b$ and

investigate how iterative refinement from Section 2.3 can be employed to solve this system. Let us first introduce some notation.

Let \widehat{u}_h be the approximation of the discrete solution u_h to Problem 3.1 such that

$$\widehat{u}_h(\cdot, \omega) = \sum_{j=1}^n \widehat{x}_j(\omega) \phi_j \quad (6)$$

and let $r(\omega) := A(\omega)\widehat{x}(\omega) - b(\omega)$ denote the residual.

Lemma 3.2. *Let u_h be the discrete solution of Problem 3.1 and let \widehat{u}_h be the approximation of u_h defined above. Then*

$$\|u_h(\cdot, \omega) - \widehat{u}_h(\cdot, \omega)\|_{H_0^1(D)} \leq C \|f(\cdot, \omega)\|_{L^2(D)} \frac{\|r(\omega)\|_2}{\|b(\omega)\|_2} \quad \text{for a.e. } \omega \in \Omega,$$

where C is independent of h , u , and ω and $\|\cdot\|_2$ denotes the Euclidean norm on \mathbb{R}^n .

Proof. For $\omega \in \Omega$ fixed, the bound follows from [13, Proposition 9.19], with a constant independent of u and h . To see that C is also independent of ω , we write out the constant C from [13, Proposition 9.19] explicitly:

$$C = \frac{\kappa(\mathcal{M}_t)^{1/2}}{c_P \alpha}. \quad (7)$$

Here, c_P is the Poincaré constant, α is the coercivity constant of the bilinear form \mathcal{A} and $\kappa(\mathcal{M}_t)$ is the condition number of the mass matrix \mathcal{M}_t . It follows from the definition of \mathcal{M}_t that $\kappa(\mathcal{M}_t)$ is independent of ω ; see [13, Section 9.1.3]. Due to (4), the coercivity constant α is also independent of ω . This completes the proof. \square

Thus, to control the error $\|u_h(\cdot, \omega) - \widehat{u}_h(\cdot, \omega)\|_{H_0^1(D)}$ it suffices to control the relative residual $\|r(\omega)\|_2 / \|b(\omega)\|_2$ of the resulting linear system. In the following we derive the convergence rate of iterative refinement from Section 2.3 applied to the FE system from Problem 3.1. This will guide our choice of the precisions in iterative refinement (Algorithm 2.1). To proceed with our analysis, we need some auxiliary inequalities from [13], which we summarize here.

Lemma 3.3. *Let $A(\omega)x(\omega) = b(\omega)$ be the FE system corresponding to the approximate FE solution \widehat{u}_h of Problem 3.1 as in (6). The following estimates hold:*

1. $\|A(\omega)\|_2 \leq c$, and
2. $\kappa_2(A(\omega)) \leq ch^{-2}$,

where κ_2 is the condition number of A with respect to the spectral norm and the generic constant c is independent of the discretisation parameter h and of ω .

Proof. The first claim follows from the proof of [13, Theorem 9.11] (the last inequality in the first part) together with [13, Theorem 9.8]. The inequality from [13, Theorem 9.11] gives us a bound on $\|A\|_2$ using h and the eigenvalues of the mass matrix, which then can be bounded using [13, Theorem 9.8].

The second claim follows from [13, Theorem 9.11] (with $s = t = 1$) as well as [13, Example 9.13]. The ω -independence of the constant c follows as in Lemma 3.2 from the definition of the stiffness matrix A and from (4). \square

As a consequence of Lemma 3.3 we formulate the following corollary about convergence properties of iterative refinement for the FE systems. It follows immediately from [7, Corollary 4.2] using the inequalities from Lemma 3.3 and the fact that $\|x(\omega)\|_2 \leq \|A^{-1}(\omega)\|_2 \|b(\omega)\|_2$. For the purpose of this corollary we make the reasonable assumption that $\|\widehat{x}_i(\omega)\|_2 \approx \|x(\omega)\|_2$.

Corollary 3.4. *Let ϕ be the approximate convergence rate of iterative refinement applied to the FE system $A(\omega)x(\omega) = b(\omega)$ corresponding to Problem 3.1. The solution eventually computed by Algorithm 2.1 is denoted by $\widehat{x}_i(\omega)$. Then*

1. *the factor ϕ satisfies $\phi \leq c\varepsilon_s(1 + h^{-2})$ and*

$$2. \frac{\|b(\omega) - A(\omega)\widehat{x}_i(\omega)\|_2}{\|b(\omega)\|_2} \leq cp_z\varepsilon(1 + h^{-2}),$$

with generic constants derived from [7, Corollary 4.2] and Lemma 3.3.

This corollary allows us to analyse convergence properties of iterative refinement for our model problem. In particular, for a given value of the tolerance δ_e , we are able to derive upper bounds on the precisions ε_r , ε , and ε_f in Algorithm 2.1 (recall that in our case $\varepsilon_s = \varepsilon_f$). The convergence rate ϕ has to be “sufficiently smaller than 1” with the exact meaning of this statement given in [7, Theorem 4.1]. The first bound in Corollary 3.4, thus leads to an upper bound for the factorisation precision ε_f . Using the second bound in Corollary 3.4, it is sufficient to set $cp\varepsilon(1 + h^{-2}) < \delta_e$, which yields a bound on the working precision ε . The residual precision only needs to satisfy the condition $\varepsilon_r \leq \varepsilon$, so that we can set $\varepsilon_r = \varepsilon$. Under these constraints on ε_r , ε , and ε_f , [7, Corollary 4.2] guarantees that Algorithm 2.1 converges and Corollary 3.4 provides a bound on the convergence rate ϕ .

4 Inexact computations in multilevel Monte Carlo

4.1 Standard multilevel Monte Carlo

Multilevel Monte Carlo (MLMC) is one of the standard multilevel sampling methods to compute expectations for uncertainty quantification (UQ) in PDE applications, and a suitable example to show how inexact computations can be leveraged in that context. The main idea of MLMC is to optimally balance the sampling and discretisation errors of a hierarchy of approximate models; see [15] for an overview. We formulate it here in full generality:

Suppose $Q : \Omega \rightarrow \mathbb{R}$ is a random variable and we are interested in computing its mean $\mathbb{E}[Q]$. Assume that Q cannot be evaluated sample-wise, but a sequence of models $Q_l, l \in \{0, \dots, N\}$, approximating Q with increasing accuracy, is available. We define the following auxiliary Monte Carlo (MC) estimators:

$$\widehat{Y}_0 := \frac{1}{N_0} \sum_{k=1}^{N_0} Q_0^{(k)} \quad \text{and} \quad \widehat{Y}_l := \frac{1}{N_l} \sum_{k=1}^{N_l} (Q_l^{(k)} - Q_{l-1}^{(k)}),$$

where $l = 1 \dots, L$. The estimator

$$\widehat{Q}_{L, \{N_l\}}^{\text{ML}} := \sum_{l=0}^L \widehat{Y}_l \tag{8}$$

will then be referred to as the MLMC estimator for $E[Q]$. Although not necessary, the estimators \widehat{Y}_l are, in this work, assumed to be independent. In this definition, it is assumed that the models can be evaluated *exactly*, i.e., we can compute $Q_l(\omega)$. In the following we sometimes abuse notation and denote by $\widehat{Q}_{L, \{N_l\}}^{\text{ML}}$ an estimate computed using the estimator $\widehat{Q}_{L, \{N_l\}}^{\text{ML}}$.

In practice, we use an adaptive algorithm to determine the values L and $\{N_l\}_{l=0}^L$ for a given tolerance TOL; see [10, Section 2]). The adaptive MLMC algorithm aims to compute the optimal values of L and $\{N_l\}_{l=0}^L$ by minimizing the computational cost for a given variance. To this end, the algorithm uses sample averages \widehat{Y}_l (see (8)) and variance estimators

$$s_l^2 := \frac{1}{N_l} \sum_{k=1}^{N_l} (Y_l^{(k)} - \widehat{Y}_l)^2 \tag{9}$$

of the random variables $\{Y_l\}_{l=0}^L$. What we also need in the algorithm is the cost C_l to evaluate $Q_l(\omega)$ for each sample $\omega \in \Omega$.

The MLMC complexity can be analysed by imposing standard assumptions on Q and Q_l . Namely, we assume that there exists $m > 1$ and $\alpha, \beta, \gamma > 0$ such that

$$|\mathbb{E}[Q_l - Q]| = O(m^{-\alpha l}), \quad \text{var}[Y_l] = O(m^{-\beta l}), \quad \text{and} \quad C_l = O(m^{\gamma l}). \quad (10)$$

It can be shown that three complexity regimes can be distinguished based on the values of β and γ . The optimal performance of the MLMC algorithm is achieved when $\beta > \gamma$, i.e., when variance decays faster than cost increases. The full complexity analysis can be found in [10, Theorem 1].

4.2 Computational error in multilevel Monte Carlo

In this section we present a convergence analysis taking into account the computational error in the MLMC method discussed in Section 4.1. Our analysis shows that especially on the coarser levels, it is sufficient to compute with relatively low effective precision. It suggests that significant gains in terms of both memory and computational time can be obtained depending on the model considered and its implementation. To this end, we propose a novel adaptive MLMC algorithm, which determines the minimum required numerical precision with no additional cost. This algorithm will be referred to as *mixed precision multilevel Monte Carlo (MPML)* for simplicity. The efficiency of the adaptive algorithm is demonstrated on numerous experiments in Section 5.

Let us start by defining the setting. As in Section 4.1, we assume $Q : \Omega \rightarrow \mathbb{R}$ to be a random variable and the goal is to compute its mean $\mathbb{E}[Q]$. This time we assume that we cannot evaluate $Q_l(\omega)$ exactly, but only an approximation \tilde{Q}_l of Q_l . This might be due to finite precision arithmetic for the model evaluation or for generating the random variable. Using \tilde{Q}_l instead of Q_l in the MLMC estimator (8) gives us what will be referred to as the mixed precision multilevel Monte Carlo estimator and will be denoted by $\hat{Q}_{L, \{N_l\}}^{\text{MPML}}$. The crucial difference between the MPML estimator and the standard MLMC estimator is the error model which is used. For MPML we propose an additive error model stated below. Using the bias-variance decomposition we can also quantify the overall error of the MPML estimator.

Theorem 4.1 (Computational error in MPML). *Let $m \in \mathbb{N}$, $m > 1$ and assume that $\delta_0, \delta_1, \dots$ is a sequence of parameters characterising computational error with $1 > \delta_l > 0$. Assume that there exist $\alpha_1, \beta_1, \alpha_2, \beta_2 > 0$ such that*

$$|\mathbb{E}[\tilde{Q}_l - Q]| = O(m^{-\alpha_1 l} + \delta_l^{\alpha_2}), \quad (11)$$

$$\text{var}[\tilde{Y}_l] = O(m^{-\beta_1 l} + \delta_l^{\beta_2}). \quad (12)$$

Let $L \in \mathbb{N}$ and $N_0, \dots, N_L \in \mathbb{N}$ and let $\hat{Q}_{L, \{N_l\}}^{\text{MPML}}$ be the corresponding MPML estimator. Then, the MSE of this estimator satisfies

$$\mathbb{E}[(\mathbb{E}[Q] - \hat{Q}_{L, \{N_l\}}^{\text{MPML}})^2] \leq C \left(\left(m^{-2\alpha_1 L} + \sum_{l=0}^L \frac{m^{-\beta_1 l}}{N_l} \right) + \left(m^{-\alpha_1 L} \delta_L^{\alpha_2} + \delta_L^{2\alpha_2} + \sum_{l=0}^L \frac{\delta_l^{\beta_2}}{N_l} \right) \right).$$

Proof. The inequality follows straightforwardly from the bias-variance decomposition (see [10]) and the assumptions (11) and (12). \square

This general error estimate can be used in practice to compute a bound on the computational error so that the overall MSE does not exceed a certain tolerance. A concrete example of what form the parameter δ_l can take will be discussed in the next section. For the purpose of this general error estimate we have not assumed that the computational error decays. An example of this would be the situation when we have a hierarchy of approximations of a linear PDE and solve the resulting system of linear algebraic equations

on each level using an iterative solver with a fixed number of iterations, or a sparse direct solver in finite precision. Then the error of the model decays with increasing l , but we expect the computational error to grow. This is in accordance with what has been observed in [16, Figure 3.1].

4.3 Application to the elliptic PDE problem

In this section we show how the abstract analysis of computational error in MLMC from Section 4.2 can be applied to the elliptic PDE problem. The precise problem statement is the following:

Problem 4.2. Let $G : H_0^1(D) \rightarrow \mathbb{R}$ be a bounded linear functional and consider Problem 3.1, an AVP with random data and solution $u(\cdot, \omega) \in H_0^1(D)$ for a.e. $\omega \in \Omega$. We consider the problem of estimating the quantity of interest (QoI) defined as the expected value of the random variable $Q : \Omega \rightarrow \mathbb{R}$ given by $\omega \mapsto G(u(\cdot, \omega))$.

Under assumptions (4) and (5), it can be shown that when MLMC is applied to Problem 4.2, we obtain (10) with $\alpha = 2$ and $\beta = 4$. Generally γ depends on the linear solver used and we discuss it in our numerical experiments. If an optimal linear solver is used (e.g., multigrid), one has $\gamma = 2$; see [10].

Throughout this section we will use the symbol \hat{u}_h to denote the discrete solution of the AVP with random data (Problem 3.1) expanded in the FE basis as in (6) with \hat{x} computed effectively to precision δ such that

$$\frac{\|b(\omega) - A(\omega)\hat{x}(\omega)\|_2}{\|b(\omega)\|_2} \leq C\delta. \quad (13)$$

The constant $C > 0$ is independent of the problem data and ω . The validity of this assumption in practice is discussed at the end of Section 4.4.

In our PDE problem, we assume a hierarchy of discrete models based on a uniform refinement with a factor $m > 1$ of an initial mesh with mesh size h_0 . Assumptions (11) and (12) may then be rewritten as

$$|\mathbb{E}[\tilde{Q}_l - Q]| = O(h_l^{\alpha_1} + \delta_l^{\alpha_2}), \quad \text{and} \quad \text{var}[\tilde{Y}_l] = O(h_l^{\beta_1} + \delta_l^{\beta_2}). \quad (14)$$

The values of the constants α_1 , α_2 , β_1 , and β_2 are given by the following lemma.

Lemma 4.3. *Let $m > 1$, and let h_0, h_1, \dots be discretisation parameters satisfying $h_0 > 0$ and $mh_l = h_{l-1}$. Let \hat{u}_{h_l} be the discrete solution of the AVP with random data (Problem 3.1) computed effectively to precision δ_l on mesh level l , and assume that there are $k_1, k_2 > 1$ such that $k_1\delta_l \leq \delta_{l-1} \leq k_2\delta_l$ for all $l \geq 1$. Then*

$$|\mathbb{E}[\tilde{Q}_l - Q]| = O(h_l^2 + \delta_l), \quad (15)$$

$$\text{var}[\tilde{Y}_l] = O(h_l^4 + \delta_l^2). \quad (16)$$

Proof. Using Jensen's inequality the bias error in (15) can be decomposed as

$$\begin{aligned} |\mathbb{E}[\tilde{Q}_l - Q]| &\leq \mathbb{E}[|G(\hat{u}_{h_l}) - G(u)|] \\ &= \|G(u) - G(u_{h_l}) + G(u_{h_l}) - G(\hat{u}_{h_l})\|_{L^1(\Omega, \mathbb{R})} \\ &\leq \|G(u) - G(u_{h_l})\|_{L^1(\Omega, \mathbb{R})} + \|G(u_{h_l}) - G(\hat{u}_{h_l})\|_{L^1(\Omega, \mathbb{R})}, \end{aligned} \quad (17)$$

From [10, Section 3] it follows that

$$\|G(u) - G(u_h)\|_{L^1(\Omega, \mathbb{R})} \leq Ch^2, \quad (18)$$

where $C > 0$ is independent of h , u , and ω . Since G is bounded and \hat{u}_h is computed effectively to precision δ , it follows from Lemma 3.2 that

$$|G(u_h(\cdot, \omega)) - G(\hat{u}_h(\cdot, \omega))| \leq C\|f(\cdot, \omega)\|_{L^2(D)}\delta,$$

with a generic constant $C > 0$ independent of u , h , and ω . Integrating this inequality over Ω yields $\|G(u_h) - G(\hat{u}_h)\|_{L^1(\Omega, \mathbb{R})} \leq C\delta$, which combined with (18) and (17) gives us the desired bound on the bias error in (15).

The variance bound in (16) can be shown similarly. Let us estimate

$$\begin{aligned} \text{var}[\tilde{Y}_l] &= \mathbb{E}[\tilde{Y}_l^2] - \mathbb{E}[\tilde{Y}_l]^2 \\ &\leq \mathbb{E}[(\tilde{Q}_l - Q_{h_l} + Q_{h_l} - Q + Q - Q_{h_{l-1}} + Q_{h_{l-1}} - \tilde{Q}_{l-1})^2]. \end{aligned} \quad (19)$$

Using the same technique as in [10], we obtain an estimate of the form

$$\begin{aligned} \text{var}[\tilde{Y}_l] &\leq C(\mathbb{E}[(\tilde{Q}_l - Q_{h_l})^2] + \mathbb{E}[(Q_{h_l} - Q)^2] \\ &\quad + \mathbb{E}[(Q - Q_{h_{l-1}})^2] + \mathbb{E}[(Q_{h_{l-1}} - \tilde{Q}_{l-1})^2]). \end{aligned} \quad (20)$$

As in [10], the quantity $\mathbb{E}[(Q_{h_l} - Q)^2] + \mathbb{E}[(Q - Q_{h_{l-1}})^2]$ can be estimated by

$$\mathbb{E}[(Q_{h_l} - Q)^2] + \mathbb{E}[(Q - Q_{h_{l-1}})^2] \leq Ch_l^4. \quad (21)$$

To bound the other two terms in (20) we proceed as follows: As above, since G is bounded and \hat{u}_{h_l} is computed effectively to precision δ_l , Lemma 3.2 gives

$$|G(u_{h_l}(\cdot, \omega)) - G(\hat{u}_{h_l}(\cdot, \omega))| \leq C\|f(\cdot, \omega)\|_{L^2(D)}\delta_l,$$

for a generic constant $C > 0$ independent of u , h_l , and ω . Taking the second power of this inequality and integrating over Ω yields

$$\|G(u_{h_l}) - G(\hat{u}_{h_l})\|_{L^2(\Omega, \mathbb{R})}^2 \leq C\delta_l^2, \quad (22)$$

Similarly, $\|G(u_{h_{l-1}}) - G(\hat{u}_{h_{l-1}})\|_{L^2(\Omega, \mathbb{R})}^2 \leq C\delta_{l-1}^2 \leq Ck_2^2\delta_l^2$. Together with (20), (21) and (22) this yields the desired estimate (16). \square

This lemma allows us to formulate a specific version of Theorem 4.1 regarding the error of the MPML estimator applied to Problem 4.2 discretised using finite elements. We summarize this in the following corollary.

Corollary 4.4 (Error of the MPML FEM). *Let the assumptions of Lemma 4.3 be satisfied. Let $L \in \mathbb{N}$ and $N_0, \dots, N_L \in \mathbb{N}$ and let $\hat{Q}_{L, \{N_l\}}^{MPML}$ be the corresponding MPML estimator. Then the MSE of this estimator satisfies*

$$\mathbb{E}[(\mathbb{E}[Q] - \hat{Q}_{L, \{N_l\}}^{MPML})^2] \leq C \left(\left(h_L^4 + \sum_{l=0}^L \frac{h_l^4}{N_l} \right) + \left(h_L^2 \delta_L + \delta_L^2 + \sum_{l=0}^L \frac{\delta_l^2}{N_l} \right) \right).$$

Proof. The claim follows from Lemma 4.3 and Theorem 4.1. \square

In this section we have not focused on the cost of the MPML method. This is because the asymptotic cost remains the same as for the standard MLMC method as long as $\delta_L = O(h_L^\alpha)$ and $\delta_l^2 = O(h_l^\beta)$. However, due to the use of inexact solvers, significant time and memory gains can be obtained.

4.4 Adaptive MPML algorithm

In this section we develop an adaptive algorithm which will automatically choose a suitable effective precision on each level of the MLMC method. We will use the standard MLMC algorithm as the foundation for our proposed algorithm. The first step is the choice of the target effective precision.

In order to choose the correct effective precision in each step, we will use the error bound for the MPML method from Theorem 4.1. For simplicity, we assume the bias and variance decay as in (14). We

propose the following approach: choose the accuracy δ_l on level l such that the total MSE of the MPML estimator is not greater than a constant times the MSE of the standard MLMC estimator for a fixed constant $k_p \in (0, 1)$, the choice of which we discuss later. According to Theorem 4.1, for this to hold it suffices to choose δ_l , $l = 0, \dots, L$ such that

$$h_L^{\alpha_1} \delta_L^{\alpha_2} + \delta_L^{2\alpha_2} + \sum_{l=0}^L \frac{\delta_l^{\beta_2}}{N_l} \leq k_p \left(h_L^{2\alpha_1} + \sum_{l=0}^L \frac{h_l^{\beta_1}}{N_l} \right)$$

for a fixed constant $k_p \in (0, 1)$. To balance the terms in the error estimate, it is sufficient to choose δ_l , $l = 0, \dots, L$ such that

$$h_L^{\alpha_1} \delta_L^{\alpha_2} + \delta_L^{2\alpha_2} \leq k_p h_L^{2\alpha_1} \quad \text{and} \quad \sum_{l=0}^L \frac{\delta_l^{\beta_2}}{N_l} \leq k_p \sum_{l=0}^L \frac{h_l^{\beta_1}}{N_l}. \quad (23)$$

Since for $\delta_L^{\alpha_2} < h_L^{\alpha_1}$, we have $\delta_L^{2\alpha_2} \ll h_L^{\alpha_1} \delta_L^{\alpha_2}$, it suffices to choose

$$\delta_L \leq \left(k_p h_L^{\alpha_1} \right)^{1/\alpha_2}.$$

Moreover, in order to satisfy (23) we can choose δ_l as

$$\begin{aligned} \delta_l &:= \left(k_p h_l^{\beta_1} \right)^{1/\beta_2}, \quad l = 0, \dots, L-1, \\ \delta_L &:= \min \left\{ \left(k_p h_L^{\beta_1} \right)^{1/\beta_2}, \left(k_p h_L^{\alpha_1} \right)^{1/\alpha_2} \right\}. \end{aligned} \quad (24)$$

With this choice, both inequalities in (23) are satisfied and we obtain the desired error estimate if the rest of the assumptions in Theorem 4.1 are satisfied. The reason we “hide” the computational error rather than optimally balancing it with the model error in our adaptive algorithm is that in the case when the computational error comes from a linear solver, it typically decays exponentially with the number of iterations (e.g., in iterative refinement; see Section 2.3) and therefore balancing the two errors would not bring great benefits. However, it might be of interest in cases when the computational error decreases polynomially.

Let us discuss in more detail the choice of the constant k_p . Although in this work the constant k_p is chosen to be fixed, more general choices are possible, one of which is discussed in the next paragraph. Note that the accuracy δ_l defined by (24) is, for $l < L$, not sensitive with respect to the changes of the constant k_p . Indeed, if the constant is decreased 100×, the target accuracy decreases only 10× for our model problem; see Theorem 4.4. The value $k_p := 0.05$ is a safe choice to bound the computational error, as demonstrated in Section 5. Note also that the values of δ_l can be computed “on the fly” with no additional cost, given that the decay rates of bias and variance in Theorem 4.1 are known. We now proceed to the formulation of the MPML algorithm, given in Algorithm 4.1.

It is natural to ask how the choice of the constant k_p affects the number of samples N_l required on each level l to achieve the desired tolerance. According to Theorem 4.1, if the accuracy δ_l is chosen according to (24) then the variance is increased on each level at most by approximately the factor $(1 + k_p)$. This means that the number of samples N_l on each level is increased at most by the same factor $(1 + k_p)$; see step 7 of Algorithm 4.1 Since $k_p \ll 1$, this does not pose a problem for us. Depending on the exact settings of the problem (on the linear solver), it might make sense to use a different cost model for MPML than for MLMC to estimate the cost per sample C_l on each level, which may impact the number of samples on each level as well. However, in Figure 3 we verify numerically that in our example the overall increase in the number of samples compared to standard MLMC is negligible.

Algorithm 4.1 Adaptive MPML algorithm

Require: $m, \text{TOL}, L = 1, L_{\max}, N_0 = N_1 = N_{\text{init}}$ **Ensure:** $\hat{Q}_{L, \{N_l\}}^{\text{MPML}}, \{N_l\}$

```
1: while  $L \leq L_{\max}$  do
2:   Compute  $\delta_l, l = 0, \dots, L$ , using (24)
3:   for  $l = 0$  to  $L$  do
4:     Compute  $N_l$  new samples  $Y_l^{(k)}$  using (8) with computational accuracy  $\delta_l$ 
5:     Compute  $\hat{Y}_l, s_l^2$  and estimate  $C_l$ 
6:   end for
7:   Update estimates for  $N_l$  as  $N_l := \sqrt{\frac{V_l}{C_l}} \frac{2}{\text{TOL}^2} \sum_{k=0}^L \sqrt{V_k C_k}$ 
8:   if  $|\hat{Y}_L| > \frac{rm^\alpha - 1}{\sqrt{2}} \text{TOL}$  then
9:      $L := L + 1$ 
10:     $N_L := N_{\text{init}}$ 
11:  end if
12:  if  $|\hat{Y}_L| \leq \frac{rm^\alpha - 1}{\sqrt{2}} \text{TOL}$  and  $\sum_{l=0}^L s_l^2 / N_l \leq \text{TOL}^2 / 2$  then
13:     $\hat{Q}_{L, \{N_l\}}^{\text{MPML}} := \sum_{l=0}^L \hat{Y}_l$ 
14:  end if
15: end while
```

Throughout this section we have assumed that we are able to compute the approximate discrete solution \hat{u}_{h_l} on the level l effectively to precision δ_l . How to achieve this, depends on the inexact solver that is used for the linear system. We discuss here two basic cases, iterative and direct solvers. First, any suitable iterative solver can in principle be used with the stopping criterion given by (13). Since the values of δ_l obtained using the adaptive MPML algorithm are typically relatively “big” (see Section 5 for examples), the iterative solver can potentially achieve the tolerance in a very small number of iterations, leading to significant cost gains. In this case, the cost gain does not come primarily from using low precision, but rather from reducing the number of iterations. As an example, we employ MINRES; see Section 2.2.

The second technique we propose to use, is iterative refinement. It is used here in combination with a direct solver based on Cholesky factorisation. Iterative refinement can, however, be used in principle with any direct or iterative solver; see Section 2.3 and [7]. As explained in Section 2, iterative refinement helps us to achieve just the desired accuracy with a small additional cost.

4.5 Cost analysis

The cost gain using the adaptive MPML algorithm from Section 4.4 depends on which of the three complexity regimes of the MLMC estimator in [10, Theorem 1] applies. These depend on the relative sizes of β and γ in (10).

Intuitively, one obtains the most significant gains in cases where the cost on the coarser levels dominates. This is due to the fact that on the coarser levels the discretisation error is larger and therefore the estimator can also tolerate a larger computational error without affecting the overall accuracy; see (24). The cost on the coarser levels dominates in the case when $\beta > \gamma$ in (10), i.e., when variance decays faster than the cost increases (see below for a more precise statement).

The abstract cost analysis is done here in terms of arbitrary cost units. In applications, we may consider, e.g., CPU time, memory references, or floating point operations, depending on what best fits our purpose. At the end of this subsection we apply the abstract cost analysis to the Problem 4.2 and give a concrete example of cost measures for this problem.

For the purpose of the abstract analysis we assume the following. For the standard MLMC we assume

$\text{var}[Y_l] = c_v m^{-\beta l}$ and $C_l = c_c m^{\gamma l}$ with $\beta > \gamma$; see (10) and [10, Theorem 1]. Further, we assume that both MLMC and MPML algorithms use the same number of samples N_l on each level and the variance on each level $\text{var}[Y_l]$ is the same for both algorithms. This is a reasonable assumption, since our adaptive MPML algorithm chooses the computational error significantly smaller than the model error (see the discussion in Section 4.4 and Figure 3). For the costs per sample on each level with low accuracy we assume only that

$$C_0^{\text{MP}} \leq q C_0, \quad C_l^{\text{MP}} \leq C_l, \quad l \geq 1, \quad (25)$$

where $q \in (0, 1)$ is the factor by which the coarsest level cost is reduced.

The total cost per level in MLMC decays as

$$\frac{C_{l+1} N_{l+1}}{C_l N_l} = m^{\frac{\gamma-\beta}{2}}, \quad (26)$$

where we used the definition of N_l from step 7 of Algorithm 4.1 and the bias and variance decay rates. We see that indeed the coarsest level cost dominates in the regime $\beta > \gamma$. For the total cost of the MLMC algorithm we get

$$C^{\text{ML}} = \sum_{l=0}^L C_l N_l = C_0 N_0 \frac{1 - (m^{\frac{\gamma-\beta}{2}})^L}{1 - m^{\frac{\gamma-\beta}{2}}}.$$

In summary, using (25), the ratio of the total costs of the two estimators is therefore bounded by

$$\frac{C^{\text{MPML}}}{C^{\text{ML}}} \leq q \frac{1 - m^{\frac{\gamma-\beta}{2}}}{1 - (m^{\frac{\gamma-\beta}{2}})^L} + m^{\frac{\gamma-\beta}{2}} \frac{1 - (m^{\frac{\gamma-\beta}{2}})^{L-1}}{1 - (m^{\frac{\gamma-\beta}{2}})^L}.$$

Letting $L \rightarrow \infty$ we obtain an asymptotic bound $\frac{C^{\text{MPML}}}{C^{\text{ML}}} \leq q + m^{\frac{\gamma-\beta}{2}}(1 - q)$. For $\beta > \gamma$ this bound is less than 1. We summarize this in the following corollary.

Corollary 4.5. *Assume that by using MPML (Algorithm 4.1), the computational cost on the coarsest level is reduced by a factor $q \in (0, 1)$ and that doing so does not (significantly) change the number of samples or the variance on any level compared to standard MLMC. If the variance decays sufficiently fast, i.e., $\beta > \gamma$, then the total cost of MPML is reduced asymptotically as $L \rightarrow \infty$ by at least a factor $q + m^{\frac{\gamma-\beta}{2}}(1 - q)$ compared to standard MLMC.*

By standard MLMC we mean Algorithm 4.1 without step 2, where the computations in step 4 are carried out with an a-priori given, level-independent, and sufficiently high accuracy. In our numerical experiments we always describe precisely what accuracy we chose.

As an example, consider Problem 4.2 with uniform mesh refinement by a factor of $m = 2$. Using an optimal linear solver (e.g., multigrid), we have $\gamma = 2$ and the variance of Y_l decays with a rate of $\beta = 4$ (see [10]). If $q = 1/4$, for example, then Corollary 4.5 predicts that the cost is reduced by at least a factor of 1.6. In our experiments, using the MINRES method, we observed an actual cost gain in terms of floating point operations by a factor of ≈ 1.5 (see Figure 2). When a low precision sparse direct solver with iterative refinement is used, the reduction in allocated memory is reduced by up to a factor of ≈ 3.5 (see Figure 8).

5 Numerical results

We provide numerical experiments demonstrating the potential cost savings of the adaptive MPML algorithm (Algorithm 4.1) over a standard adaptive MLMC algorithm. The adaptive MPML algorithm preserves the overall computational accuracy. As a suitable model, we use an elliptic PDE with lognormal random coefficients with both a direct and an iterative linear solver. All numerical experiments are implemented in Python. The codes are available at <https://github.com/josef-martinek/mpml>.

$k_p = 0.05$					
L	δ_0	δ_1	δ_2	δ_3	δ_4
1	3.5e-3	1.9e-4	-	-	-
2	3.5e-3	8.7e-4	4.9e-5	-	-
3	3.5e-3	8.7e-4	2.2e-4	1.2e-5	-
4	3.5e-3	8.7e-4	2.2e-4	5.5e-5	3.1e-6

l	precision values
0	<i>hhss</i>
1	<i>ssss</i>
2+	<i>ssdd</i>

Table 1: Left: Required effective precision on each level (in terms of relative residual), determined by the adaptive MPML algorithm (Algorithm 4.1) for different values of the finest level L . Right: Choice of precision values $(\varepsilon_f, \varepsilon_7, \varepsilon, \varepsilon_r)$ for iterative refinement on each level l . The factorisation is carried out in half precision on level 0.

5.1 Elliptic PDE with lognormal coefficients – iterative solver

We will solve an equation of the following form, which is a special case of (3):

$$\begin{aligned} -\nabla \cdot (a(\cdot, \omega) \nabla u(\cdot, \omega)) &= f \quad \text{on } D, \\ u(\cdot, \omega) &= 0 \quad \text{on } \partial D, \end{aligned} \tag{27}$$

for a given random field a and a deterministic right-hand side f . The random field is chosen in such a way that it corresponds to a truncated Karhunen-Loève expansion of a suitable covariance operator, in particular,

$$a(x_1, x_2, \omega) = \exp \left(\sum_{j=1}^s \omega_j \frac{1}{j^q} \sin(2\pi j x_1) \cos(2\pi j x_2) \right). \tag{28}$$

Here $\omega = (\omega_1, \dots, \omega_s) \in \mathbb{R}^s$ is such that $\omega_j \sim N(0, \sigma^2)$ for a fixed $\sigma > 0$. Random fields of this form are widely used; see [1], [27], and [10] for examples.

As the quantity of interest we choose

$$\mathbb{E}[Q] = \int_{\Omega} \left(\int_D u(x_1, x_2, \omega) d(x_1, x_2) \right) d\omega.$$

Due to the fact that $\omega_j \sim N(0, \sigma^2)$, assumptions (4) and (5) are not satisfied. By choosing, e.g., $\omega_j \sim \text{Uni}(0, c)$, one could ensure that both assumptions are satisfied, but we want to test the developed methods in a more realistic setting. The analysis in Section 3.2 could easily be extended to this setting, using the analysis for MLMC presented in [31], but we did not present this here to avoid unnecessary technicalities.

In the first example of this section, we choose the data in (27) as follows. The right-hand side satisfies $f \equiv 1$ on D and the parameters in the coefficient function are chosen as $s = 4$, $q = 2$, and $\sigma = 2$. To solve this problem numerically, we discretise (27) using the FEM as described in Section 3 with simplicial elements implemented in FEniCSx [2]. In this experiment, the discretisation parameter on the coarsest mesh is $h_0 = 1/8$ and the mesh is refined on each level by a factor $m = 2$.

Recall that in all our experiments we refer to standard MLMC as Algorithm 4.1 without step 2, where the computations in step 4 are carried out with an a-priori given, sufficiently high accuracy. In each experiment we always describe precisely what this accuracy is. For MLMC, the parameters α and β in the MLMC complexity theorem [10, Theorem 1] (see also (10)) can be chosen to be $\beta = 4$, $\alpha = 2$ for the random field in (28). To set up the MPML algorithm (Algorithm 4.1), we further need the parameters α_1 , α_2 , β_1 , and β_2 from the MPML complexity theorem (Theorem 4.1). As shown in Lemma 4.3, we have $\alpha_1 = \alpha = 2$, $\beta_1 = \beta = 4$, $\alpha_2 = 1$, and $\beta_2 = 2$. In both adaptive algorithms, the underlying linear systems are solved using the PETSc implementation of MINRES [11] with a stopping criterion given by the relative residual norm. The tolerances for the stopping criterion in the MPML algorithm are given in

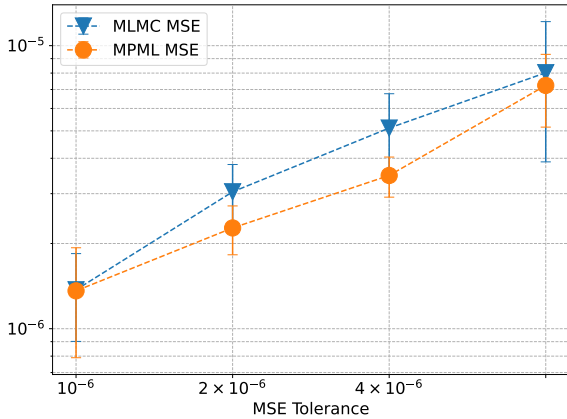


Figure 1: Estimated MSE with approximate 95% confidence intervals for the MPMC estimator when compared to the reference MLMC estimator for various target tolerances. As their linear solver, both estimators use MINRES; MPML uses an adaptively chosen stopping criterion.

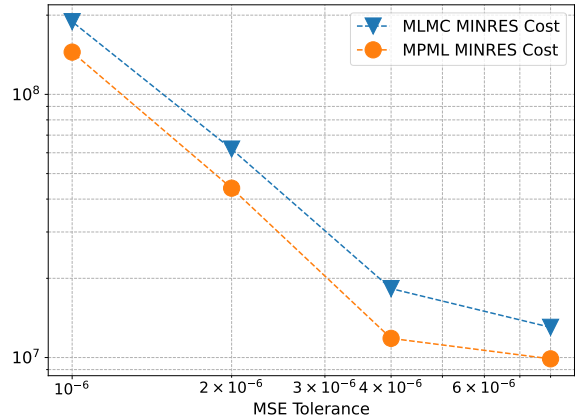


Figure 2: Total cost gain in terms of FLOPs for various tolerances using adaptive MPML compared to the standard adaptive MLMC estimator. As their linear solver, both estimators use MINRES; MPML uses an adaptively chosen stopping criterion.

Table 1 (left). The standard MLMC algorithm uses a fixed tolerance specified below for each experiment and all computations are carried out in double precision without iterative refinement. The cost of solving the linear system is estimated in terms of the number of floating point operations (FLOPs) performed by MINRES. To count the FLOPs we use the PETSc GetFlops() function.

To determine the effective precision δ_l in the MPML adaptive algorithm, we use formula (24) with the constant $k_p = 0.05$. As discussed below and depicted in Figure 4, the MPML algorithm is not sensitive with respect to the choice of k_p . For a multilevel estimator with a given number of levels, the choice of $k_p = 0.05$ then determines uniquely the effective precisions δ_l on all levels according to (24). The values of δ_l for different estimators can be found in Table 1 (left).

We now aim to verify the accuracy of the MPML algorithm. We execute 1000 runs of the adaptive MPML algorithm (Algorithm 4.1) for each of the four values of the MSE tolerance TOL^2 , namely $TOL^2 = 8, 4, 2, 1 \times 10^{-6}$. For the same tolerances we perform 1000 runs of the standard MLMC algorithm. The standard MLMC algorithm uses a fixed tolerance of 10^{-6} for the MINRES stopping criterion. Figure 1 shows the MSE of the estimates obtained by both algorithms averaged over the number of runs with approximate 95% confidence intervals. To estimate the MSE of both algorithms a reference value of the QoI is computed by the standard MLMC algorithm with tolerance $TOL^2 = 2 \times 10^{-8}$ and a direct, double precision linear solver. Up to statistical errors, both estimators have a similar MSE. However, they do differ slightly, due to the discrete choices in the two adaptive procedures, e.g., of the total number of levels L .

In Figure 2, we demonstrate the cost gains obtained by MPML (Algorithm 4.1) compared to standard MLMC, again with a fixed tolerance of 10^{-6} in the MINRES stopping criterion. We plot the average cost in terms of FLOPs for each tolerance and observe that it is consistently reduced by a factor of ≈ 1.5 . As demonstrated in Figure 1, this cost gain comes with no statistically significant loss of accuracy. It results from the fact that the effective precision δ_l for solving the linear systems on the coarser levels is chosen significantly larger than 10^{-6} in MPML, see Table 1 (left).

At the beginning of the cost analysis in Section 4.5 we made the assumption that the numbers of samples on each level are chosen approximately the same within the MPML and the MLMC adaptive procedures. We verify numerically that this is true. Figure 3 shows the average number of samples obtained by MPML

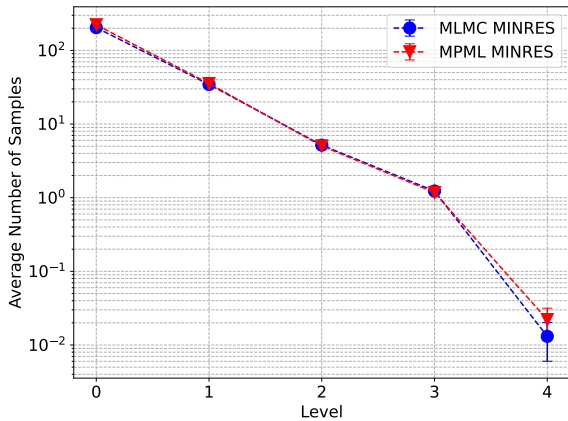


Figure 3: Average number of samples on each level for adaptive MLMC and adaptive MPML for $TOL^2 = 10^{-6}$ (with approximate 95% confidence intervals).

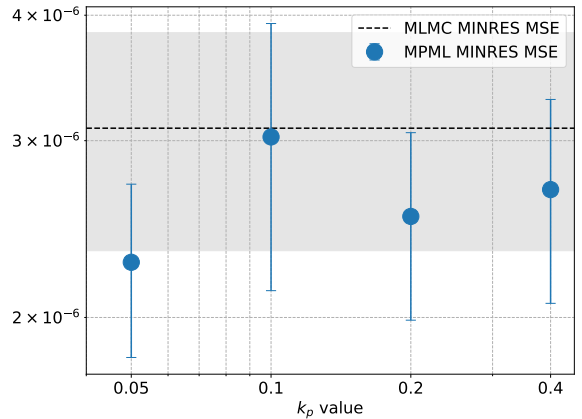


Figure 4: MSE of the MPML algorithm for various values of k_p compared to the reference MSE of MLMC (with approximate 95% confidence intervals).

(Algorithm 4.1) and standard MLMC on each level for the tolerance $TOL^2 = 10^{-6}$. We observe that the number of samples are equal within statistical error given by the approximate 95% confidence intervals. For this experiment, the standard MLMC algorithm uses a fixed tolerance of 10^{-10} in the MINRES stopping criterion. Note that Level 4 is not reached in all runs and we need on average only one sample on Level 3.

In Section 4.4 we claimed that the MPML algorithm is not sensitive to the a-priori chosen constant k_p used to determine the required computational accuracy. Figure 4 shows the average MSE of the MPML algorithm (Algorithm 4.1) for the MSE tolerance $TOL^2 = 2 \times 10^{-6}$ with approximate 95% confidence intervals. The MSE is estimated using 1000 runs of the algorithm for the values $k_p = 0.05, 0.1, 0.2, 0.4$. The estimated MSE of the standard MLMC algorithm is shown for comparison with a dashed line. It is estimated using 1000 runs of standard MLMC with a tolerance of 10^{-10} in the MINRES stopping criterion. The choice of the constant k_p seems to have no significant impact on the overall accuracy, provided the constant is chosen sufficiently small. For our suggested choice of $k_p = 0.05$ the computational error in our model problem is bounded safely.

5.2 Elliptic PDE with lognormal coefficients – direct solver

In this section, we again solve (27) with the same input data, i.e., $f \equiv 1$, $s = 4$, $q = 2$, and $\sigma = 2$. The coarsest mesh size is again $h_0 = 1/8$. However, here the underlying linear system (with symmetric positive definite matrix) is solved using a double precision Cholesky factorisation from PETSc in the standard MLMC algorithm and a low precision Cholesky factorisation with iterative refinement in our MPML algorithm. Recall that throughout our experiments by standard MLMC we mean Algorithm 4.1 without step 2, where the computations in step 4 are (here) carried out with double precision. We use our own implementation of iterative refinement and of the low precision Cholesky factorisation. To carry out computations in half, single, and double precision, we use the numerical types of NumPy, namely float16(), float32(), and float64() for half, single, and double precision, respectively. Apart from the linear solver, all calculations are carried out in double precision.

The iterative refinement (Algorithm 2.1) is set up as follows. As in the previous section, the actual, numerical values in the stopping criterion are given by the required effective precisions δ_l on each level, specified by formula (24). To this end, we also choose again $\alpha_1 = \alpha = 2$, $\beta_1 = \beta = 4$, $\alpha_2 = 1$, and $\beta_2 = 2$. Table 1 (left) shows the resulting values of the effective precision δ_l . Table 1 (right) shows the exact setting of the other precisions used in the iterative refinement algorithm. The algorithm contains 3 precisions,

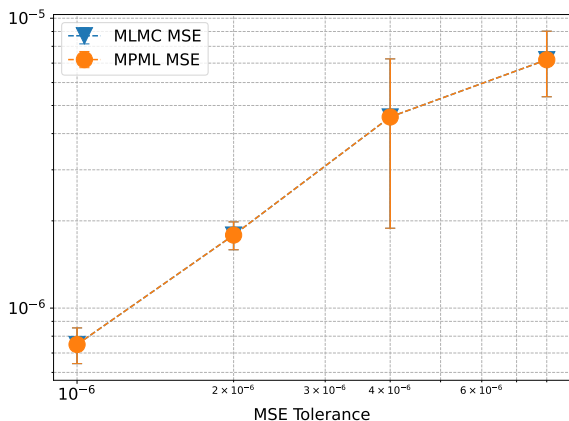


Figure 5: Comparison of estimated MSE for MPML and MLMC using the same number of samples and the same random seeds (with approximate 95% confidence intervals). MLMC uses double precision Cholesky, while MPML uses low precision Cholesky with iterative refinement.

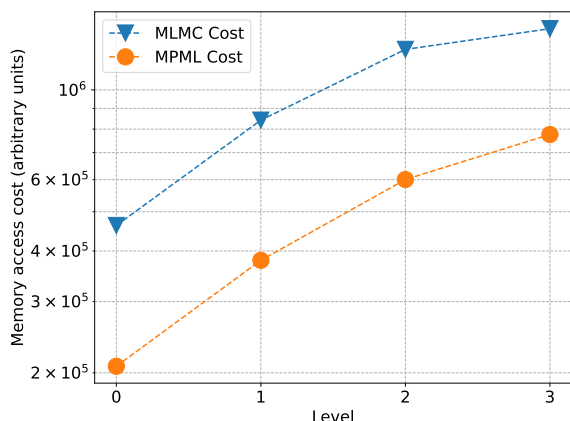


Figure 6: Comparison of total costs of the estimators per level in terms of memory access for MPML and MLMC. MLMC uses double precision Cholesky, while MPML uses low precision Cholesky with iterative refinement.

i.e., ε_f , ε , and ε_r , each taking on one of the values quarter (q), half (h), single (s), or double (d). To simplify the notation, we describe the exact setting of the iterative refinement schematically as an ordered quadruple, e.g., $(\varepsilon_f, \varepsilon_8, \varepsilon, \varepsilon_r) = (hhs)$, where ε_8 is the precision chosen at step 8 of Algorithm 2.1.

In the cost model (10) we choose $\gamma = 2$. In 2D, this corresponds to the case when the linear system is solved in linear complexity, since the number of unknowns grows quadratically with the mesh size.

We start again by determining the accuracy of the MPML estimator $\hat{Q}_{L, \{N_l\}}^{\text{MPML}}$, using the setting as described above, and we compare it to the accuracy of the standard MLMC estimator $\hat{Q}_{L, \{N_l\}}^{\text{ML}}$ with double precision Cholesky as the linear solver on all levels. We perform 1000 runs of the MPML estimator and of the MLMC estimator for each of the MSE tolerances $\text{TOL}^2 = 8, 4, 2, 1 \times 10^{-6}$. To eliminate randomness from estimating the MSE and to get a better idea of how big the computational error actually is, we use the same numbers of samples in the MPML and MLMC estimators and the same seeds in the random number generators. The number of samples $\{N_l\}$ we use for both estimators is determined by 1000 runs of the standard adaptive MLMC algorithm. Figure 5 shows the resulting average mean squared errors of the MPML and MLMC estimators. The difference in the MSEs of both estimators is very small; in fact the relative error of the MPML MSE with respect to the MLMC MSE is less than 0.01%. Recall that the MPML estimator uses half and single precision for the matrix factorisation on all levels; see Table 1 (right). This promises significant memory savings when implemented efficiently on an architecture where half precision computations are supported.

We continue by estimating the cost gains using MPML estimator $\hat{Q}_{L, \{N_l\}}^{\text{MPML}}$ with low precision Cholesky factorisation and iterative refinement compared to standard MLMC estimator $\hat{Q}_{L, \{N_l\}}^{\text{ML}}$ with double precision Cholesky. Again, both estimators use the same numbers of samples $\{N_l\}$. Since memory references are by far the most costly part on modern computing architectures, both in terms of time and energy cost (cf. the discussion Section 2.4), we use memory access as a simple cost model, in terms of total number of bits loaded into main memory. Thus, accessing a half precision floating point number is $2\times$ cheaper than accessing a single precision number and $4\times$ cheaper than accessing a double precision number. The simulated cost gain can then be estimated by counting the number of entries in all vectors and the number of non-zeros in all sparse factorisations of the matrices computed and stored in the process of solving the linear systems during the iterative refinement process. Figure 6 shows the total cost gain per level (cost

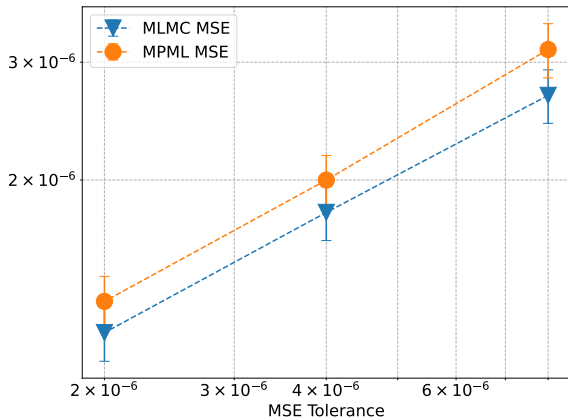


Figure 7: Comparison of estimated MSE for MPML and MLMC using the same number of samples and the same random seeds (with approximate 95% confidence intervals). MLMC uses double precision Cholesky, while MPML uses low precision Cholesky with iterative refinement (here with quarter precision on level 0).

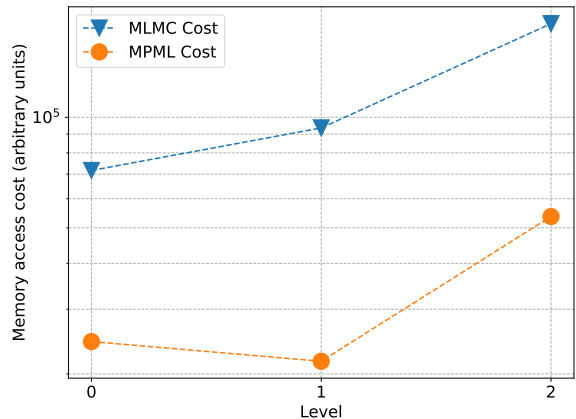


Figure 8: Comparison of total costs of the estimators per level in terms of memory access for MPML and MLMC. MLMC uses double precision Cholesky, while MPML uses low precision Cholesky with iterative refinement (here with quarter precision on level 0).

per sample \times number of samples) for $\widehat{Q}_{L,\{N_i\}}^{\text{MPML}}$ compared to $\widehat{Q}_{L,\{N_i\}}^{\text{ML}}$. On all levels we observe a simulated memory gain of ≈ 2 . The total memory gain (sum over all levels) is ≈ 2 as well.

In the last example, we show how further memory gains can be obtained using quarter precision on the coarsest level. For this experiment, we again solve (27) with $f \equiv 1$ on D , $s = 1$ and $\sigma = 1$, but now we choose the coarsest mesh size to be $h_0 = 1/4$. To determine the effective precision δ_l in (24) we choose $k_p = 0.4$. Iterative refinement with the Cholesky solver is used with the following settings: qh on level 0, and h on levels 1 to 3. This means that on level 0 where $h_0 = 1/4$, quarter precision (q43, see Section 2.1) is used for the Cholesky factorisation. To simulate quarter precision, the `pychop` package of Xinye Chen was used; see [8]. Figures 7 and 8 show the MSE for MPML and MLMC and the simulated memory gain, respectively. They have been produced analogously to Figures 5 and 6. We observe that for the MSE tolerance 2×10^{-6} , the MPML relative error is 11% bigger compared to standard MLMC error with the same number of samples, while we are able to achieve a total memory gain of ≈ 3.5 . Recall that the cost gain is simulated by counting non-zeros computed and stored in the process of solving the linear system $Ax = b$.

We have not encountered overflow in any of the examples presented in this section when working with the lower precisions. It is important to note that due to the fact that the coefficients of the PDE are lognormally distributed, overflow can occur with low probability. In the case where overflow occurs, scaling or shifting techniques can be used; see [23].

6 Conclusion

Multilevel sampling methods have proven to be powerful tools for uncertainty quantification, offering significant performance improvements by efficiently redistributing computational work across a hierarchy of models. In this paper, we demonstrated how leveraging computations of lower accuracy on coarser levels can further enhance the efficiency of these methods in high-performance computing applications. As a use case, we have developed an adaptive algorithm to determine the minimum required computational accuracy for each level in the multilevel Monte Carlo method.

Through two practical examples, we showcased the potential of our approach to obtain significant cost gains. Using a low-precision sparse direct solver with iterative refinement, we achieved a simulated memory gain of up to $3.5\times$, while employing a MINRES iterative solver yielded a speedup of $2\times$ in floating point operations. These results highlight the significant potential for energy-aware scientific computing. The potential for future work lies in generalising this approach to other uncertainty quantification frameworks, such as multilevel Markov chain Monte Carlo or the multilevel stochastic collocation method and exploring its broader applications in scientific computing. The efficient parallel implementation of low-precision solvers within multilevel sampling methods is of great interest and promises to bring further speedup.

Acknowledgements

This work is supported by the Carl Zeiss-Stiftung through the project “Model-Based AI: Physical Models and Deep Learning for Imaging and Cancer Treatment” and by the Deutsche Forschungsgemeinschaft (German Research Foundation) under Germany’s Excellence Strategy EXC 2181/1 - 390900948 (the Heidelberg STRUCTURES Excellence Cluster). The second author is supported by the Charles University Research Centre program No. UNCE/24/SCI/005 and the European Union (ERC, inEXASCALE, 101075632). Views and opinions expressed are those of the authors only and do not necessarily reflect those of the European Union or the European Research Council. Neither the European Union nor the granting authority can be held responsible for them.

References

- [1] I. Babuška, R. Tempone, and G. E. Zouraris. “Galerkin finite element approximations of stochastic elliptic partial differential equations”. In: *SIAM Journal on Numerical Analysis* 42.2 (2004), pp. 800–825.
- [2] I. A. Baratta et al. *DOLFINx: The next generation FEniCS problem solving environment*. <https://doi.org/10.5281/zenodo.10447666>. Dec. 2023. DOI: [10.5281/zenodo.10447666](https://doi.org/10.5281/zenodo.10447666). URL: <https://doi.org/10.5281/zenodo.10447666>.
- [3] A. Barth, C. Schwab, and N. Zollinger. “Multi-level Monte Carlo finite element method for elliptic PDEs with stochastic coefficients”. In: *Numerische Mathematik* 119 (2011), pp. 123–161.
- [4] C. Brugger et al. “Mixed precision multilevel Monte Carlo on hybrid computing systems”. In: *2014 IEEE Conference on Computational Intelligence for Financial Engineering & Economics (CIFER)*. IEEE, 2014, pp. 215–222.
- [5] E. Carson. *Communication-Avoiding Krylov Subspace Methods in Theory and Practice*. University of California, Berkeley, 2015.
- [6] E. Carson and N. J. Higham. “A new analysis of iterative refinement and its application to accurate solution of ill-conditioned sparse linear systems”. In: *SIAM Journal on Scientific Computing* 39.6 (2017), A2834–A2856.
- [7] E. Carson and N. J. Higham. “Accelerating the solution of linear systems by iterative refinement in three precisions”. In: *SIAM Journal on Scientific Computing* 40.2 (2018), A817–A847.
- [8] X. Chen. *pychop: A Python package for simulating low-precision arithmetic*. <https://pypi.org/project/pychop/>. Accessed: 2025-01-30. 2025. URL: <https://pypi.org/project/pychop/>.
- [9] J. A. Christen and C. Fox. “Markov Chain Monte Carlo Using an Approximation”. In: *Journal of Computational and Graphical Statistics* 14.4 (2005), pp. 795–810. ISSN: 10618600. URL: <http://www.jstor.org/stable/27594150> (visited on 09/21/2024).

- [10] K. A. Cliffe et al. “Multilevel Monte Carlo methods and applications to elliptic PDEs with random coefficients”. In: *Computing and Visualization in Science* 14 (2011), pp. 3–15.
- [11] L. D. Dalcin et al. “Parallel distributed computing using Python”. In: *Advances in Water Resources* 34.9 (2011). New Computational Methods and Software Tools, pp. 1124–1139. ISSN: 0309-1708. DOI: [10.1016/j.advwatres.2011.04.013](https://doi.org/10.1016/j.advwatres.2011.04.013).
- [12] W. J. Dally, Y. Turakhia, and S. Han. “Domain-specific hardware accelerators”. In: *Communications of the ACM* 63.7 (2020), pp. 48–57.
- [13] A. Ern and J.-L. Guermond. *Theory and Practice of Finite Elements*. Vol. 159. Springer, 2004.
- [14] R. A. Freeze. “A stochastic-conceptual analysis of one-dimensional groundwater flow in nonuniform homogeneous media”. In: *Water Resources Research* 11.5 (1975), pp. 725–741.
- [15] M. B. Giles. “Multilevel Monte Carlo methods”. In: *Acta Numerica* 24 (2015), pp. 259–328.
- [16] M. B. Giles and O. Sheridan-Methven. “Rounding Error Using Low Precision Approximate Random Variables”. In: *SIAM Journal on Scientific Computing* 46.4 (2024), B502–B526. DOI: [10.1137/23M1552814](https://doi.org/10.1137/23M1552814).
- [17] A. Greenbaum. *Iterative Methods for Solving Linear Systems*. SIAM, 1997.
- [18] A. Haidar et al. “Harnessing GPU tensor cores for fast FP16 arithmetic to speed up mixed-precision iterative refinement solvers”. In: *SC18: International Conference for High Performance Computing, Networking, Storage and Analysis*. IEEE. 2018, pp. 603–613.
- [19] A. Haidar et al. “The design of fast and energy-efficient linear solvers: On the potential of half-precision arithmetic and iterative refinement techniques”. In: *International Conference on Computational Science*. Springer. 2018, pp. 586–600.
- [20] S. Heinrich. “Multilevel Monte Carlo methods”. In: *Large-Scale Scientific Computing: Third International Conference, LSSC 2001 Sozopol, Bulgaria, June 6–10, 2001 Revised Papers 3*. Springer. 2001, pp. 58–67.
- [21] N. J. Higham. *Accuracy and stability of numerical algorithms*. SIAM, 2002.
- [22] N. J. Higham and T. Mary. “Mixed precision algorithms in numerical linear algebra”. In: *Acta Numerica* 31 (2022), pp. 347–414.
- [23] N. J. Higham, S. Pranesh, and M. Zounon. “Squeezing a matrix into half precision, with an application to solving linear systems”. In: *SIAM Journal on Scientific Computing* 41.4 (2019), A2536–A2551.
- [24] R. J. Hoeksema and P. K. Kitanidis. “Analysis of the spatial structure of properties of selected aquifers”. In: *Water Resources Research* 21.4 (1985), pp. 563–572.
- [25] M. Horowitz. “1.1 computing’s energy problem (and what we can do about it)”. In: *IEEE International Solid-State Circuits Conference (ISSCC), Digest of Technical Papers*. IEEE. 2014, pp. 10–14.
- [26] N. P. Jouppi et al. “Ten lessons from three generations shaped Google’s TPuv4i”. In: *Proceed. 48th Annual International Symposium on Computer Architecture (ISCA ’21)*. Virtual Event, Spain: IEEE Press, 2021, pp. 1–14. ISBN: 9781450390866. DOI: [10.1109/ISCA52012.2021.00010](https://doi.org/10.1109/ISCA52012.2021.00010).
- [27] F. Nobile, R. Tempone, and C. G. Webster. “A sparse grid stochastic collocation method for partial differential equations with random input data”. In: *SIAM Journal on Numerical Analysis* 46.5 (2008), pp. 2309–2345.
- [28] NVIDIA Corporation. *NVIDIA H100 Tensor Core GPU Architecture*. URL: <https://resources.nvidia.com/en-us-tensor-core>. [Accessed 23-4-2023]. URL: [URL : %20https : //resources.nvidia.com/en-us-tensor-core](https://resources.nvidia.com/en-us-tensor-core).
- [29] A. E. Scheidegger. *The Physics of Flow through Porous Media*. University of Toronto Press, 1957.

- [30] A. L. Teckentrup et al. “A multilevel stochastic collocation method for partial differential equations with random input data”. In: *SIAM/ASA Journal on Uncertainty Quantification* 3.1 (2015), pp. 1046–1074.
- [31] A. L. Teckentrup et al. “Further analysis of multilevel Monte Carlo methods for elliptic PDEs with random coefficients”. In: *Numerische Mathematik* 125 (2013), pp. 569–600.
- [32] B. Vieuble. “Mixed precision iterative refinement for the solution of large sparse linear systems”. PhD thesis. INP Toulouse, 2022.
- [33] T. Weinberg and B. Sousedík. “Fast implementation of mixed RT0 finite elements in MATLAB”. In: *SIAM Undergraduate Research Online* 12 (2018).